



Contents lists available at ScienceDirect

Journal of South American Earth Sciences

journal homepage: www.elsevier.com/locate/james

Late Cenozoic calc-alkaline volcanism over the Payenia shallow subduction zone, South-Central Andean back-arc (34°30'–37°S), Argentina

Vanesa D. Litvak^{a,*}, Mauro G. Spagnuolo^a, Andrés Folguera^a, Stella Poma^b,
Rosemary E. Jones^c, Víctor A. Ramos^a

^a Instituto de Estudios Andinos Don Pablo Groeber, Universidad de Buenos Aires-CONICET, Intendente Güiraldes 2160, Ciudad Universitaria, Pabellón II, C1428EHA, Buenos Aires, Argentina

^b Instituto de Geociencias Básicas y Aplicadas de Buenos Aires, Universidad de Buenos Aires-CONICET, Intendente Güiraldes 2160, Ciudad Universitaria, Pabellón II, C1428EHA, Buenos Aires, Argentina

^c Department of Earth Sciences, University of Oxford, United Kingdom

ARTICLE INFO

Article history:

Received 17 December 2014

Received in revised form

4 September 2015

Accepted 14 September 2015

Available online xxx

Keywords:

Andesitic volcanism

Shallow subduction

Back-arc

Geochemistry

San Rafael Block

ABSTRACT

A series of mesosilicic volcanic centers have been studied on the San Rafael Block (SRB), 300 km to the east of the present-day volcanic arc. K–Ar ages indicate that this magmatic activity was developed in at least two stages: the older volcanic centers (~15–10 Ma) are located in the central and westernmost part of the SRB (around 36°S and 69°W) and the younger centers (8–3.5 Ma) are located in an eastern position (around 36°S and 69°30'W) with respect to the older group. These volcanic rocks have andesitic to dacitic compositions and correspond to a high-K calc-alkaline sequence as shown by their SiO₂, K₂O and FeO/MgO contents. Elevated Ba/La, Ba/Ta and La/Ta ratios show an arc-like signature, and primitive mantle normalized trace element diagrams show typical depletions of high field strength elements (HFSE) relative to large ion lithophile elements (LILE). Rare earth element (REE) patterns suggest pyroxene and amphibole crystallization. Geochemical data obtained for SRB volcanic rocks support the proposal for a shallow subduction zone for the latest Miocene between 34°30'–37°S. Regionally, SRB volcanism is associated with a mid-Miocene to early Pliocene eastward arc migration caused by the shallowing of the subducting slab in the South-Central Andes at these latitudes, which represents the evolution of the Payenia shallow subduction segment. Overall, middle Miocene to early Pliocene volcanism located in the Payenia back-arc shows evidence for the influence of slab-related components. The younger (8–3.5 Ma) San Rafael volcanic rocks indicate the maximum slab shallowing and the easternmost extent of slab influence in the back-arc.

© 2015 Elsevier Ltd. All rights reserved.

1. Introduction

Large variations in morphology along the Andes, particularly those related to the segmentation associated with variable shortening processes, are still the focus in local and regional tectonic studies. Many of these large variations correlate with the development of arc magmatism. The geometry of the subducting slab,

and even more importantly changes in slab geometry through time, are one of the major factors that control the development, intensity and migration/expansion of volcanic arcs (Kay et al., 1991, 1999; Litvak et al., 2007; Ramos and Folguera, 2005a).

The Andes between 34° and 37°30'S consist of the Cordillera Principal and a lower mountain system to the east known as the San Rafael Block (SRB), which is separated by a Neogene foreland basin. The SRB lies in a similar longitudinal position to the Pre-cordillera, which is located to the north of the study region in the present-day Pampean flat-slab segment (Fig. 1). However, its morphology, which corresponds to a dismembered peneplain that emerges in the foreland region, and the mechanics of its exhumation, which is related to the reactivation of high-angle basement faults during Miocene to Quaternary times (Polanski, 1963;

* Corresponding author.

E-mail addresses: vane@gl.fcen.uba.ar (V.D. Litvak), maurospag@yahoo.com (M.G. Spagnuolo), andresfolguera2@yahoo.com.ar (A. Folguera), stella@gl.fcen.uba.ar (S. Poma), Rosie.Jones@earth.ox.ac.uk (R.E. Jones), andes@gl.fcen.uba.ar (V.A. Ramos).

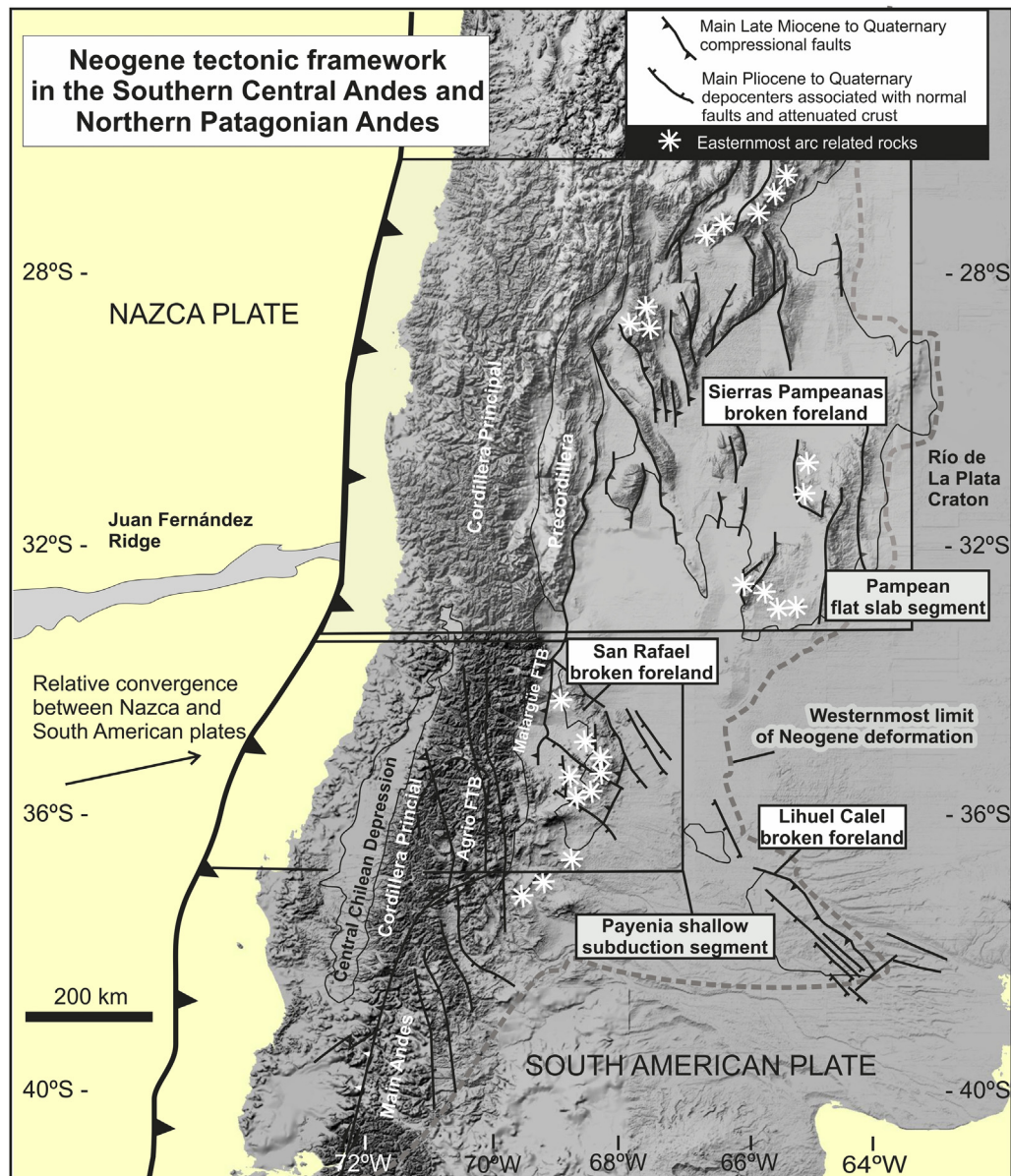


Fig. 1. The location and main morphotectonic features of the present-day Pampean flat-slab segment and the partially contemporaneous late Miocene Payenia shallow subduction zone, which is responsible for uplifting the San Rafael Block in the foreland area (locations of arc-related centers in the Pampean flat-slab segment after Ramos et al., 2002; Río de La Plata Craton after Rapela et al., 2007).

González Díaz, 1964, 1972a), makes the SRB similar to the Sierras Pampeanas. The Sierras Pampeanas are part of a broken foreland which is located to the north of the SRB and to the east of the Precordillera. Its formation has been linked to the shallowing of the subducting Nazca plate between 27° and 33°S, which started at ~17 Ma (Jordan et al., 1983; Ramos et al., 2002).

A series of andesitic to dacitic volcanic complexes has been mapped on the SRB, 300 km behind the present-day volcanic arc and in the back-arc of the Andean Southern Volcanic Zone (SVZ) (Holmberg, 1962; Polanski, 1964; González Díaz, 1964), (Fig. 2). As summarized by Dyhr et al. (2013a), evolution of the volcanism in the back-arc, in the Payenia region, can be divided into three main episodes which are differentiated according to their age, composition and tectonic setting: i) an early Miocene episode of alkaline volcanism, which is represented by the La Matancilla and Fortunoso lavas (Kay and Copeland, 2006; Kay et al., 2006b; Dyhr et al., 2013b), ii) a middle Miocene to early Pliocene episode

represented by the Palaoco, Chachahuén and Huincán volcanic sequences, which have arc-like signatures (Kay et al., 2006a,b; Nullo et al., 2002; Spagnuolo et al., 2012; Dyhr et al., 2013a) and iii) an episode of late Pliocene-Recent volcanism, which involved the eruption of alkali basalts with typical back-arc compositions and variable slab input (Bermúdez et al., 1993; Bertotto et al., 2009; Gudnason et al., 2012; Søager et al., 2013). The evolution of this volcanic activity was influenced by the shallowing of the down-going slab; the shallowing of the subduction zone is thought to have occurred between 18 and 5 Ma, with the plate at its shallowest at the time the Chachahuén sequence erupted (7.3–4.9 Ma) (Kay et al., 2006a,b).

The main focus of this work was to study the andesitic and dacitic volcanic complexes located in the easternmost back-arc position of the Payenia volcanic province, to the east of Laguna Llanquanelo (Figs. 2 and 3), with a view to examining the geochemistry and petrogenesis of the volcanism in this region. On

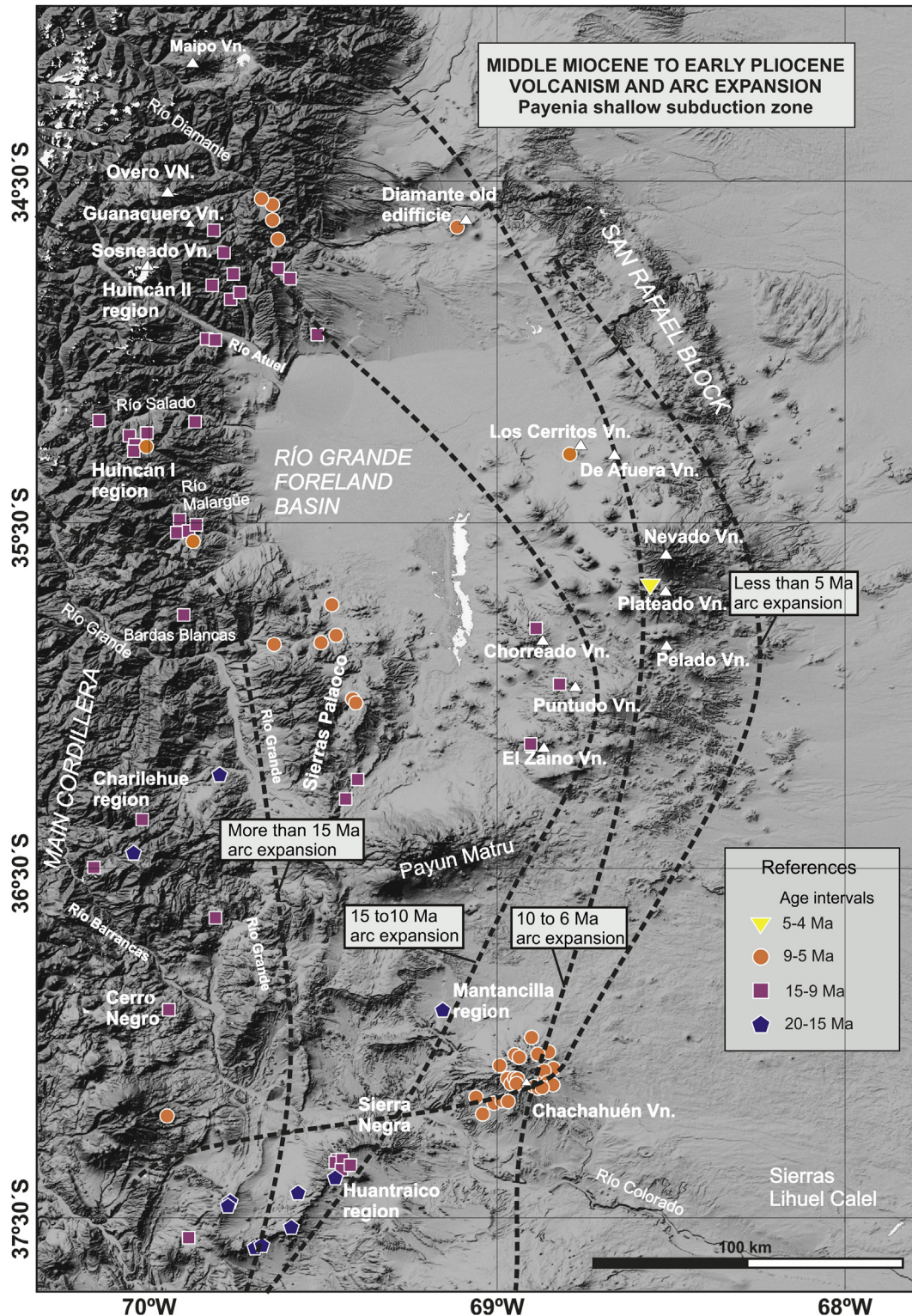


Fig. 2. Regional distribution of mesosilicic volcanic rocks from the eastern Main Andes to the San Rafael Block in the foreland area showing the eastward expansion and migration of the middle Miocene to early Pliocene arc influence in the back-arc area. Age compilation are from Nullo et al. (1993, 1999, 2002), Ramos and Barbieri (1989), Osters et al. (1999), Cobbold and Rossello (2003), Giambiagi et al. (2005), Kay and Copeland (2006), Kay et al. (2006a,b), Folguera et al. (2009), Spagnuolo et al. (2012), Dyhr et al. (2013a,b) and Ramos et al. (2014).

the basis of a recent detailed chronological study (Ramos et al., 2014), these volcanic complexes can be included in the middle Miocene to early Pliocene episode of Payenia back-arc volcanism. Here we present new geochemical data for these SRB volcanic rocks

and compare them to previously published analyses of regionally and temporally related magmatism in order to document the volcanic evolution of the Payenia province during the middle Miocene-early Pliocene. By studying the geographic position and

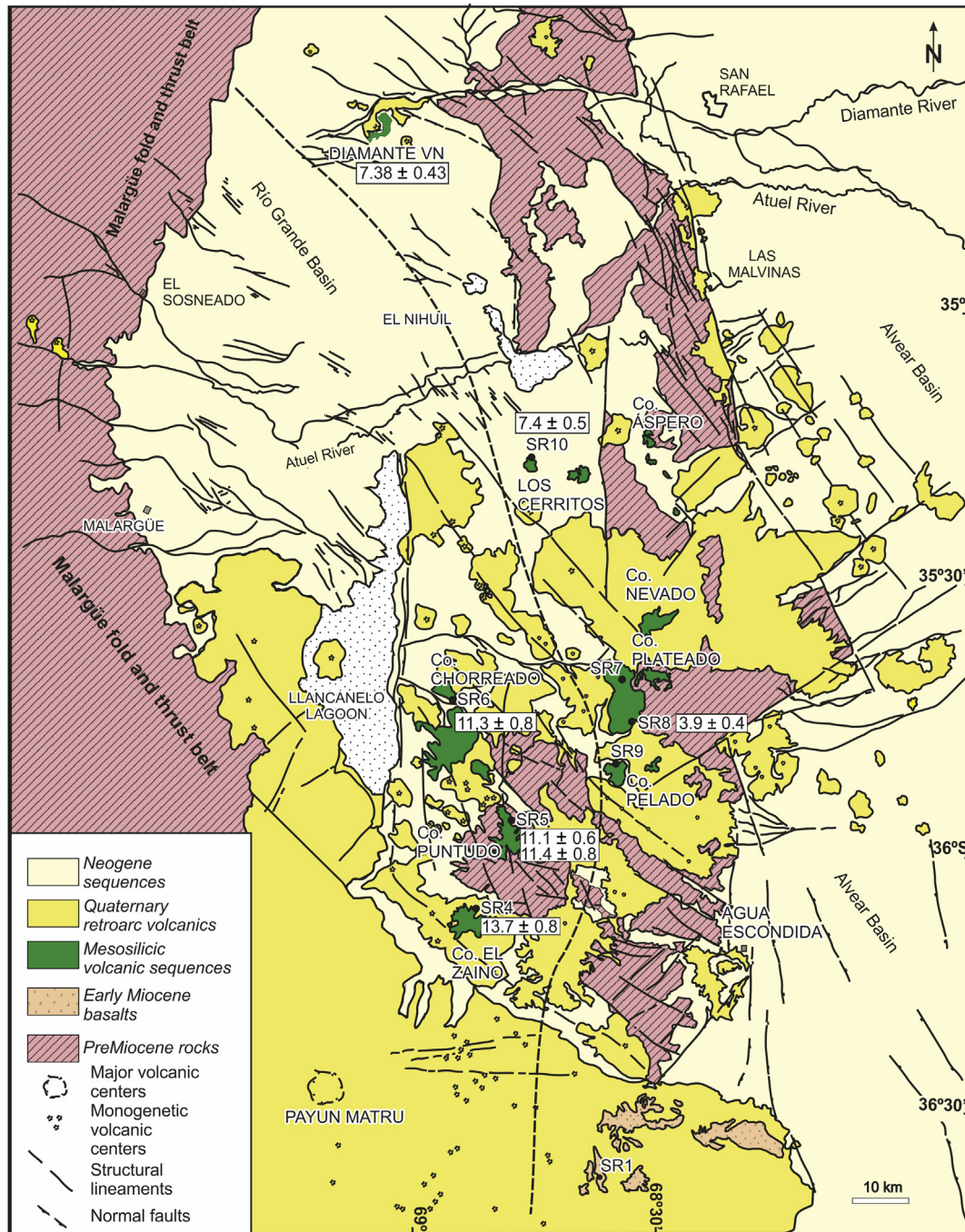


Fig. 3. Geological map of the Miocene–Pliocene mesosilicic volcanic sequences in the San Rafael Block and their relationships to pre-Miocene and post-Miocene volcanic units (after Desanti, 1956; Polanski, 1963, 1964; González Díaz, 1964, 1972a,b,c, 1979; Holmberg, 1964, 1973; Núñez, 1976a,b, 1979; Fidalgo, 1973), with sample locations indicated. A dashed line separates the distribution of San Rafael volcanics according to their age, as determined by Folguera et al. (2009) and Ramos et al. (2014).

geochemical signatures of the SRB volcanic rocks we are able to re-evaluate both the lateral expansion and latitudinal differences of the shallow subduction regime over the back-arc.

2. Regional tectonic framework

The Andes between 34° and 38°S are formed by two east-verging mountain systems, which are associated with foreland basins (Figs. 1 and 2): a) the Malargüe fold and thrust belt associated with the Río Grande basin and its continuation to the south into the Agrio fold and thrust belt, associated with smaller

synorogenic depocenters; and to the east b) the San Rafael Block whose uplift and exhumation has been associated with sedimentation in the upper section of the Alvear basin, together with other smaller basement uplifts to the southeast following the same trend, as the Sierras Lihuel Calel (Fig. 2).

During the late Oligocene to early Miocene, the westernmost sections of the Malargüe and Agrio fold and thrust belts experienced an episode of extension leading to the formation of the Abanico (Godoy et al., 1999; Charrier et al., 2002; Fock, 2005; Fock et al., 2006) and Cura Mallín (Suárez and Emparán, 1995; Radic et al., 2002; Croft et al., 2003; Burns et al., 2006; Flynn et al.,

2008) basins respectively; volcanoclastic depocenters greater than 3000 m thick. Extension was likely related to strong roll back of the subducting Nazca Plate caused by the deceleration of the South American Plate (see Rojas Vera et al., 2014 and references there in). Back-arc alkaline, volcanic successions of late Oligocene–early Miocene age accumulated further east over the southern section of the SRB at the same latitudes (González Díaz, 1979; Ramos and Barbieri, 1989; Kay et al., 2006a,b; Dyhr et al., 2013b). These back-arc successions could be associated with the intra-arc Cura Mallin and Abanico volcanic successions being emplaced to the west during the same time interval (Kay et al., 2006a,b).

The SRB and Lihuel Calel uplifted blocks were developed on the western margin of the Alvear basin, which was subsequently covered by synorogenic deposits resulting from these uplifts (Yrigoyen, 1993). The main phase of uplift of these ranges can be inferred as post-mid Miocene based on the age of the Aisol sequences, which are considered to be distal facies of the initial Río Grande basin that extensively covered the foreland area prior to the uplift of the SRB (Desanti, 1956; Polanski, 1964; González Díaz, 1972a; Soria, 1983; Yrigoyen, 1993, 1994).

The calc-alkaline intrusive bodies and volcanic sequences that constitute the focus of this work, intruded and covered the distal foreland deposits represented by the Aisol sequence (Fig. 3). This magmatism was previously assigned to Miocene times (Desanti, 1956; Polanski, 1964; González Díaz, 1972a; Núñez, 1976a,b, 1979; Marshall et al., 1986; Yrigoyen, 1994) and more recently to the middle Miocene–early Pliocene (Kay et al., 2006a,b; Dyhr et al., 2013a; Ramos et al., 2014). These middle Miocene–early Pliocene volcanic and intrusive rocks were subsequently covered by Quaternary, mafic volcanic sequences, which constitute one of the major volcanic provinces in the Andean back-arc (Fig. 3) (Groeber, 1946; Muñoz Bravo et al., 1989; Bermúdez et al., 1993; Ramos and Folguera, 2005b, 2011; Folguera et al., 2009; Llambías et al., 2010; Gudnason et al., 2012; Søager et al., 2013). Most of the volcanic vents corresponding to this magmatic stage are monogenetic, rising in the foreland area and the Malargüe orogenic front, and are associated with extensive mafic fields on their flanks (Holmberg, 1964; González Díaz, 1972b; Bermúdez et al., 1993; Bermúdez y Delpino, 1989; Rossello et al., 2002; Hernando et al., 2002, 2014; Galland et al., 2005; Llambías et al., 2010).

3. Distribution and age of middle Miocene to early Pliocene volcanic sequences

Mesosilicic volcanic sequences of mid-Miocene to early Pliocene age located in the Payenia back-arc are distributed from the eastern Malargüe fold and thrust belt to the SRB in the foreland area (Fig. 2). Most of the volcanic units in the Malargüe fold and thrust belt are between 19 and 10 Ma, while ages to the east range from ca. 14 to 4 Ma (Baldauf, 1997; Nullo et al., 2002; Giambiagi et al., 2005, 2008; Kay and Copeland, 2006; Kay et al., 2006a,b; Spagnuolo et al., 2012; Dyhr et al., 2013a,b; Ramos et al., 2014).

A series of isolated volcanic centers, which are the focus of this work, are located on the SRB and constitute the easternmost expression of back-arc volcanism in the Payenia region. Recently reported K-Ar ages indicate that this magmatic activity was developed during middle Miocene to early Pliocene times (Ramos et al., 2014). Based on the spatial distribution of the volcanic centers, we are able to distinguish two separate groups with two distinct age ranges (Fig. 3). The first group is located in the westernmost and central part of the SRB (~36°S and 69°W), and comprises three stratovolcanoes: Cerro Chorroado, Cerro Puntudo and Cerro El Zaino. Age determinations for these volcanoes range between ~15 and 10 Ma; Puntudo volcano has two K-Ar radiometric determinations of 11.1 ± 0.6 Ma (plagioclase) and 11.4 ± 0.8 Ma

(amphibole); while El Zaino and Chorroado volcanoes have K-Ar ages of 13.7 ± 0.8 Ma (whole rock) and 11.3 ± 0.8 Ma (plagioclase) respectively (Ramos et al., 2014). A second stage of volcanism is identified to the east and is comprised of younger mesosilicic volcanic centers (8–3.5 Ma) (Fig. 3). From north to south, these correspond to Los Cerritos, Cerros Plateado and Cerro Pelado volcanoes. Los Cerritos yielded a K-Ar age of 7.4 ± 0.5 Ma (plagioclase/amphibole); and an age of 3.9 ± 0.4 Ma (K-Ar on plagioclase) was obtained for Plateado volcano (Ramos et al., 2014). Lava flows from the older parts of the Diamante volcano, which is located further north (34°15'S–69°W, Fig. 3), yielded a K-Ar age of 7.4 ± 0.5 (Folguera et al., 2009), making them coeval with the younger flows present in the SRB.

San Rafael volcanic rocks are presently preserved as highly eroded stratovolcanoes. These middle Miocene–early Pliocene volcanoes were explosive and generated lava flows, alongside with pyroclastic deposits and subvolcanic bodies. The volcanic products were originally named the Cortaderas Formation (Delpino and Bermúdez, 1985; Llambías et al., 2010).

The oldest and westernmost Miocene stratovolcanoes, such as Chorroado, Puntudo and Zaino, are composite volcanoes of 2–6 km in diameter, while the younger and easternmost stratovolcanoes have smaller dimensions (1–3 km in diameter) (Figs. 3 and 4). However, Cerro Nevado, located to the north of Cerro Plateado, was developed as a complex volcanic system, the Nevado-Plateado Complex, with alkaline trachytes, trachyandesites and basalts, grouped as Nevado Formation by Bermúdez (1991), and determined to be Pliocene (Quidelleur et al., 2009; Ramos et al., 2014).

Basaltic lava flows of late Oligocene–early Miocene age (González Díaz, 1979; Kay et al., 2006a,b) underlie the mesosilicic sequences in the SRB at the southeast of the El Zaino volcano. These basalts were also sampled for geochemical purposes, in order to compare with the andesitic and dacitic sequences.

4. Analytical techniques

The samples selected for geochemical analyses are from fresh lava flows from each of the Miocene and Pliocene stratovolcanoes located within the SRB. Specifically samples were collected from the same lava flows dated by Ramos et al. (2014). Samples were prepared and analyzed at the Activation Laboratories of Ancaster, Ontario, Canada: for major elements by fusion-inductively coupled plasma (ICP) and for trace and rare earth elements by fusion-ICP Mass Spectrometry (ICP-MS). According to the laboratory procedures (<http://www.actlabs.com>) unaltered rock fragments were crushed until 90% were <2 mm. A 250 g split was then pulverized with a mild steel mill until 95% passed through a sieve with a mesh of 105 microns. For major element analysis, samples were mixed with a flux of lithium metaborate and lithium tetraborate and fused in an induction furnace. The melt was then poured into a solution of 5% nitric acid containing an internal standard, and mixed continuously until completely dissolved.

The samples were analyzed for major element oxides on a combination of simultaneous/sequential Thermo Jarrell-Ash EN-VIRO II ICP or a Varian Vista 735 ICP. Calibration was performed using 7 prepared USGS and CANMET certified reference materials. One of the 7 standards was run as unknown during the analysis of every group of ten samples. For trace element analysis, fused samples were diluted and analyzed by Perkin Elmer Sciex ELAN 6000, 6100 or 9000 ICP/MS. Three blanks and five controls (three before each sample group and two after) were analyzed per group of samples. The standards used were SY-3, NIST-694, W-2, DNC-1, BIR-1, GBW-07113, NIST-1633b and STM-1 for major elements and trace elements, plus IFG, FKN, WMG-1, MAG-1, GXR-2, LKSD-3, MICA-FE and GXR-1, also for trace elements, as reported

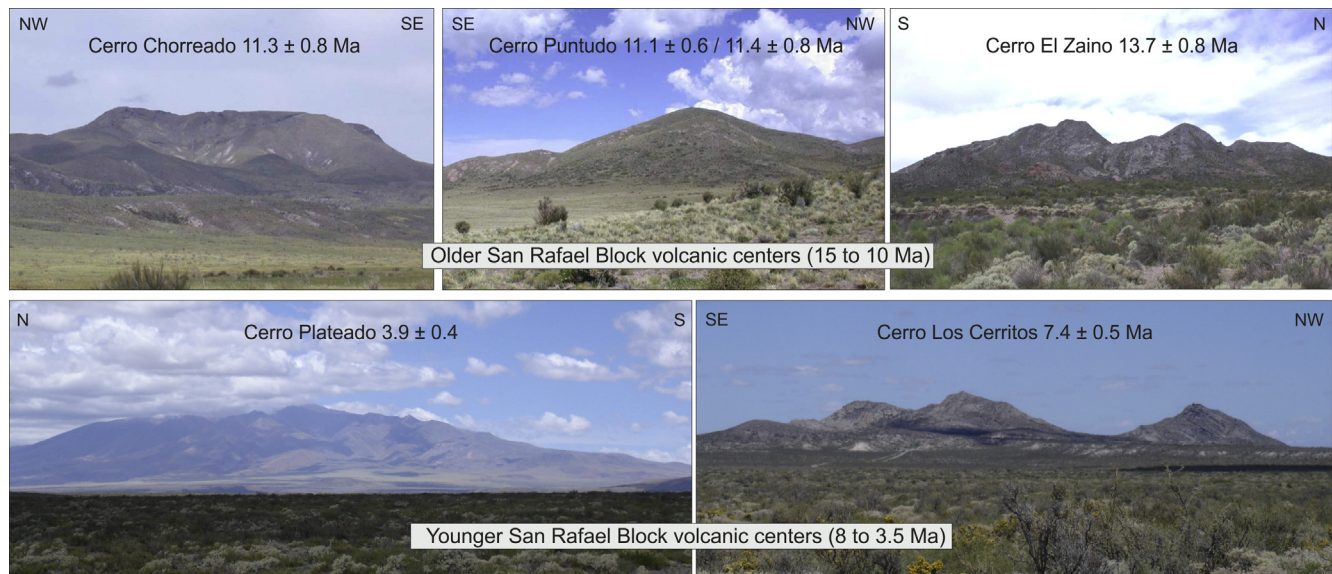


Fig. 4. Field pictures of middle Miocene to early Pliocene volcanic centers from the San Rafael Block preserved as highly eroded stratovolcanoes. See Fig. 3 for location in a plan view. Ages are from Ramos et al. (2014).

by the laboratory (see [Supplementary material](#) for results of analyzed standards). Sample locations, lithological type, and the results of major, trace and rare earth element analysis are presented in [Table 1](#), together with the detection limits of the analysis.

5. Sampling strategy and petrographic features

A regional reconnaissance of the volcanoes was undertaken in order to identify representative samples for dating, petrographical and geochemical purposes. Sample locations are shown in [Fig. 3](#) and presented in [Table 1](#). In general the lava flows are gray with porphyritic textures, containing 20–30% sub-to-euhedral phenocrysts of plagioclase and mafic minerals, which appear unaltered in hand specimen.

The mineral assemblages and textures of both the younger and older lavas are very similar; all of them show porphyritic to seriate textures with a felty groundmass ([Fig. 5](#)). Plagioclase is usually the main crystal phase and bigger phenocrysts frequently show oscillatory zoning and sieve textures on the margins of the crystals ([Fig. 5a](#) and [b](#)). Samples from both age groups have amphibole phenocrysts ([Fig. 5b](#), [d](#) and [e](#)), while pyroxene is more frequent in the older lavas (e.g., SR6 from Cerro Chorreado, [Fig. 5a](#)) and is only present in the younger lavas with more basandesitic compositions. In the older samples, amphibole is frequently replaced by opaque minerals, but in the younger samples it appears as fresh pleochroic hornblende ([Fig. 5b–e](#)).

The groundmass of the lavas is mostly felty, with interstitial tridymite commonly occurring in the more silica-rich compositions (e.g., SR7 from Cerro Plateado, SR10 from Los Cerritos). Smaller, uncolored pyroxene crystals are present in the felty matrix of the more basandesitic samples. Opaque minerals and apatite constitute the main accessory phases; abundant and euhedral brownish apatite is present as a distinguishing feature of sample SR4 (Cerro El Zaino, [Fig. 5c](#)).

Some samples, such as SR4 from El Zaino, show evidence for mixing, apparent not only by the sieve texture and zoning of plagioclase, but also by the presence of two groundmasses, one felty and another rich in tridymite and opaque minerals.

The sample from the early Miocene basaltic sequence (SR1) is an

olivine rich-basalt, with an ophitic to a subophitic texture. The olivine present in this sample is slightly altered to iddingsite, while clinopyroxene and plagioclase appear alteration free; all these mineral phases have an average grain size of 0.6 mm.

6. Results

For geochemical interpretation, the studied samples are divided into two groups according to their geographical location and the reported ages (previously described in [Section 3](#)). The older group (15–10 Ma) includes samples from El Zaino (SR4), Puntudo (SR5) and Cerro Chorreado (SR6), located in the central and westernmost part of San Rafael Block; and the younger group (8–3.5 Ma) includes samples from Cerros Plateado (SR7 and SR8), Pelado (SR9) and Los Cerritos (SR10), located in an eastern position and to the north and south of the older group ([Fig. 3](#)).

6.1. Major elements

In general, there is an overlap of both groups of lavas in major elements diagrams; only one sample from El Zaino (SR4) shows higher K₂O and FeO/MgO values that exceed the overlap field of both groups of lavas ([Fig. 6a](#)). All the samples have calc-alkaline, high-K compositions, as seen in [Fig. 6a](#) and [b](#). The older lavas are all andesites with 60–62 wt.% SiO₂, whilst the younger volcanic rocks are both more and less evolved than the older samples with SiO₂ contents ranging from 54 to 67 wt.% ([Fig. 6](#)). Sample SR9 is a basaltic andesite (54 wt.% SiO₂), SR10 is an andesite (58 wt.% SiO₂), and samples SR7 and SR 8 classify as dacites (65 and 67 wt.% SiO₂).

The chemical signature of the oldest sample (SR1, early Miocene) differs from the calc-alkaline trend shown by the previously described lavas. According to the TAS-diagram ([Le Maitre et al., 1989](#)), it classifies as an alkaline basalt (48.28 wt.% SiO₂ vs. 5.38 wt.% K₂O + Na₂O).

6.2. Trace elements and REEs

Mantle normalized trace element diagrams for the San Rafael volcanic rocks of different ages/stages of volcanism are presented in [Fig. 7](#). SRB rocks show enrichments in the LILE relative to the HFSE,

Table 1Whole rock chemical results of middle Miocene-early Pliocene back-arc volcanism in San Rafael Block.^a

San Rafael block volcanic rocks										
		D.L.	Older volcanic centers (15–10 Ma)			Younger volcanic centers (8–3.5 Ma)				Early Miocene
			Cerro Chorreado	Cerro Puntudo	Cerro El Zaino	Cerro Pelado	Cerro Los Cerritos	Cerro Plateado	Cerro Plateado	
			SR6	SR5	SR4	SR9	SR10	SR8	SR7	
			Clpx- , Hbl- bearing andesites			Hbl- bearing andesites				
SiO ₂ (wt.%)	0.01	60.39	60.74	62.19	54.14	57.79	64.89	67.17	48.28	
TiO ₂	0.01	0.634	0.608	0.597	1.032	0.599	0.336	0.258	2.303	
Al ₂ O ₃	0.01	16.87	17.07	17.25	16.72	18.69	17.76	16.65	14.68	
Fe ₂ O ₃ (T)	0.01	5.68	5.51	4.86	7.48	5.84	2.95	2.3	12.11	
MnO	0.001	0.14	0.167	0.15	0.159	0.167	0.083	0.057	0.156	
MgO	0.01	2.23	1.9	1.38	3.98	2.36	1.01	0.86	8.35	
CaO	0.01	6.21	6.19	4.85	8.28	7.73	4.1	3.32	8.36	
Na ₂ O	0.01	3.78	3.78	4.41	4.11	3.92	5.26	5.17	3.87	
K ₂ O	0.01	2.25	2.45	3.85	2.72	2.13	2.47	2.18	1.51	
P ₂ O ₅	0.01	0.27	0.32	0.29	0.43	0.31	0.19	0.14	0.63	
LOI	0.01	1.28	0.96	0.34	0.84	0.54	1.45	1.4	<0.01	
Total		99.71	99.69	100.20	99.83	100.1	100.50	99.50	99.87	
Sr (ppm)	2	708	891	893	979	1220	1228	1074	749	
Cs	0.1	2.9	4	6.8	3	1.1	2.7	2.3	0.2	
Rb	1	61	82	166	44	168	75	51	15	
Ba	3	1199	1040	976	885	921	1266	1290	300	
Th	0.05	3.38	3.1	10.3	7.11	9.19	4.35	2.76	1.98	
U	0.01	1.41	1.74	4.03	2.06	2.51	1.56	1.31	0.73	
Ta	0.01	0.66	0.79	46.2	0.81	0.46	0.49	0.4	2.62	
Nb	0.2	8.1	9.7	17.7	11.1	5.7	6.5	4.7	30.4	
Zr	1	119	149	225	145	165	152	121	171	
Hf	0.1	3.2	3.8	5.6	4	3.7	3.1	2.6	4.1	
Y	0.5	17.6	20.1	22.7	17.7	13.1	21.7	12.2	19.9	
Sc	1	12	9	5	17	13	3	3	18	
Cr	20	<20	<20	<20	90	<20	<20	<20	260	
Co	1	10	8	8	18	9	5	4	41	
Ni	20	<20	<20	<20	30	<20	<20	<20	160	
La	0.05	22.3	22	42.1	31.6	33.7	20	13.4	23.3	
Ce	0.05	43.8	46.1	77.1	61.7	64.6	38	25.2	47.6	
Pr	0.01	5.43	6.11	9.28	7.8	8.02	4.61	2.96	6.22	
Nd	0.05	21.2	24.4	33.1	30.6	29.2	17.6	10.8	26.2	
Sm	0.01	4.44	5.23	6.03	6.36	5.35	3.45	2.17	6.33	
Eu	0.005	1.51	1.76	1.74	1.97	1.57	1.09	0.708	2.19	
Gd	0.01	3.96	4.84	5.3	5.95	4.24	3.06	1.93	5.8	
Tb	0.01	0.58	0.71	0.75	0.84	0.56	0.42	0.27	0.86	
Dy	0.01	3.05	3.67	3.92	4.14	3.03	2.22	1.41	4.31	
Ho	0.01	0.6	0.71	0.75	0.76	0.6	0.4	0.27	0.74	
Er	0.01	1.73	2.06	2.26	2.14	1.83	1.18	0.78	1.89	
Tm	0.005	0.262	0.323	0.344	0.307	0.273	0.181	0.120	0.247	
Yb	0.01	1.75	2.2	2.38	2.01	1.89	1.19	0.79	1.4	
Lu	0.002	0.266	0.331	0.364	0.294	0.291	0.181	0.121	0.187	
Pb	5	17	13	19	13	15	55	21	<5	
Zn	30	70	60	60	60	40	50	<30	80	
Cu	10	10	10	10	20	30	<10	<10	40	
Ga	1	17	17	19	17	17	17	15	20	
La/Yb		12.7	10.0	17.7	15.7	17.8	16.8	17.0	16.6	
La/Sm		5.0	4.2	7.0	5.0	6.3	5.8	6.2	3.7	
Sm/Yb		2.5	2.4	2.5	3.2	2.8	2.9	2.7	4.5	
Ba/La		53.8	47.3	23.2	28.0	27.3	63.3	96.3	12.9	
Ba/Ta		1817	1316	21	1093	2002	2584	3225	115	
La/Ta		33.8	27.8	—	39.0	73.3	40.8	33.5	8.9	
Eu/Eu*		1.10	1.07	0.94	0.98	1.01	1.03	1.06	1.14	
Lat °S		35°43′05′	35°56′28′	36°04′51′	35°50′04′	35°17′04′	35°45′53′	35°40′22′	36°36′51′	
Long °W		68°52′36′	68°45′20′	68°51′47′	68°32′44′	68°44′42′	68°30′22′	68°32′53′	68°35′00′	

^a Major elements were analyzed by fusion-ICP and rare earth and trace elements by fusion ICP-MS. D.L.: Detection limits. Calculated Eu/Eu*=(EuN/√(SmN·GdN)). La/Ta value for sample SR4 was not calculated due to the anomalous value of Ta (see text).

with negative anomalies in Ta and Nb relative to La and Ce, regardless of silica content. The early Miocene basalt (SR1) shows an intraplate signature based on the enriched HFSE concentrations relative to the REEs (e.g., enrichments in Ta, Nb and, to a lesser extent, Zr (Fig. 7)), and low La/Ta ratios (8.9) (Fig. 8b).

Andesites from the older group of volcanic rocks have Ba/La ratios ranging from 23 to 54. The more mafic samples from the younger group have Ba/La ratios between 27 and 28, while the silicic samples have much higher ratios, probably related to their

higher Ba content. The Ba/Ta ratios obtained for the older volcanic rocks range from 1310 to 1820 and from 1100 to 2000 for younger samples with the same silica content. The most silica rich samples (SR8 and SR7) have higher values of 2600 and 3200. All of the samples have La/Ta values ranging between 28 and 40; except for the basaltic andesite SR10 which has a higher La/Ta ratio of 73 (Fig. 8a). Sample SR4 has anomalously high values of Ta and Nb (46.2 and 17.7 respectively) (Table 1), and therefore very low values for Ba/Ta and La/Ta. As a consequence of this anomalous

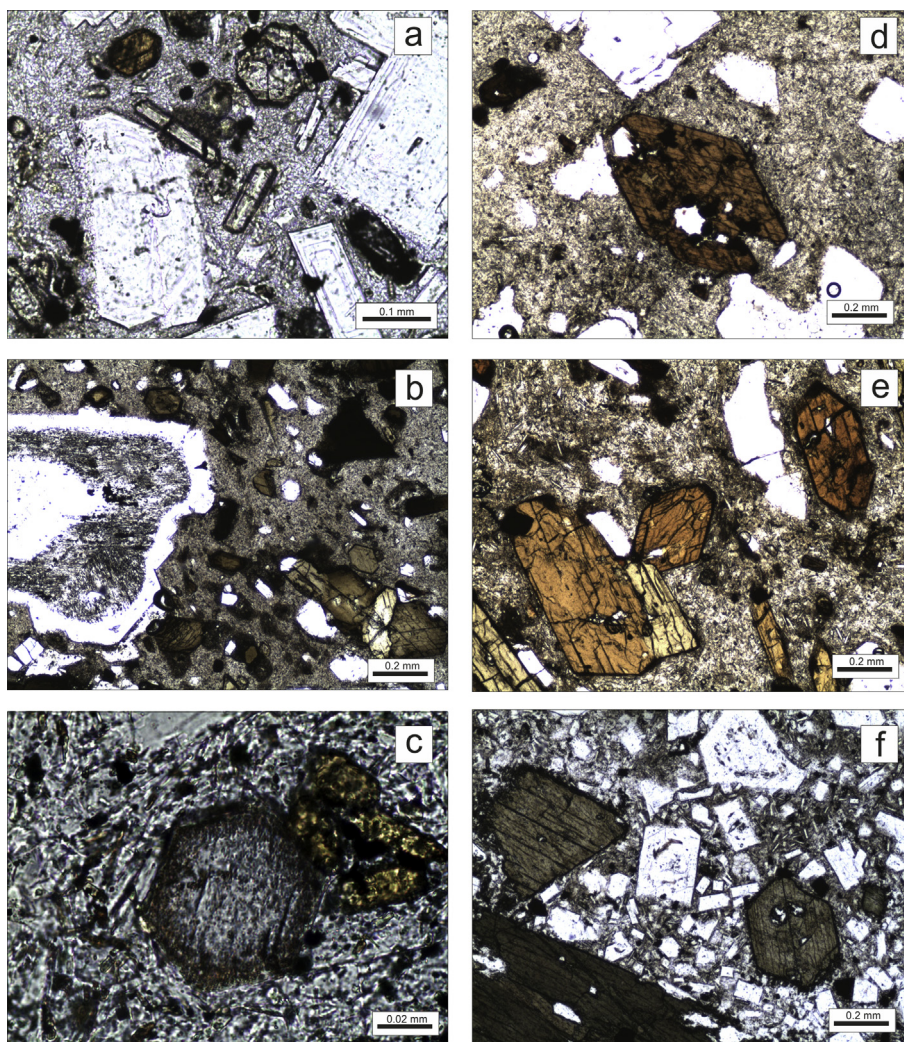


Fig. 5. Representative thin section microphotographs for the Miocene–Pliocene lavas: a) an andesite from Cerro Chorreado (SR6) showing a typical porphyritic texture with phenocrysts of plagioclase, clinopyroxene and amphibole; b) a porphyritic andesite from Cerro Puntudo (SR5) with a large plagioclase phenocryst with sieve texture; c) an andesite from Cerro El Zaino (SR4) with a felty groundmass and a brownish apatite microphenocryst; d,e) samples from Cerro Plateado (SR8–SR7) with fresh amphibole phenocrysts; f) an andesite from Cerro Los Cerritos (SR10) with a high phenocryst/groundmass ratio, with phenocrysts of plagioclase–amphibole.

value for Ta, we excluded this sample from the diagrams that include Ta.

The older volcanic rocks (SR4, SR5, SR6), which have 60–62 wt.% SiO_2 , show a moderate slope for light and heavy REE, due to their La/Sm ratios which range between 4.2 and 7.0 and their Sm/Yb ratios which range from 2.4 to 2.5 (Table 1, Fig. 7b). Silicic (SR7 and SR8) and intermediate samples (SR9, SR10) from the younger group have moderate light REE slopes (La/Sm of 5.8–6.2 and 5.0 to 6.3, respectively). However, the heavy REE slopes of the younger volcanic rocks show a steeper pattern than the older samples; silicic samples have Sm/Yb from 2.7 to 2.9, and intermediate samples from 2.8 to 3.2 (Fig. 8b, c). Neither group of samples shows negative Eu anomalies in their REE diagrams; only andesite SR4 from the older volcanic centers (cerro El Zaino) shows a weak Eu anomaly ($\text{Eu}/\text{Eu}^* = 0.94$). Eu/Eu^* obtained for the rest of the volcanic sequences range between 0.98 and 1.10 (Table 1).

Fig. 9 shows Th/Hf vs. Ta/Hf ratios of the studied volcanic rocks. The Ta/Hf values for the dacites and andesites of the younger group are relatively small compared to the andesites of the older group (0.15–0.16 vs. 0.21); except for sample SR9 which has a value of 0.20. In contrast, the older, early Miocene basalt (SR1) has a Ta/Hf value of 0.64.

7. Discussion

7.1. The development of arc-like signatures

Rare earth element patterns and phenocryst assemblages of the SRB volcanic rocks are used to gain a greater understanding into their origin and evolution. Ratios and concentrations of trace elements and REEs reflect residual minerals that are left in the source after melting or removed by fractionation processes, or could also reflect crustal assimilation processes.

In particular, fractional crystallization processes can affect the trace element compositions of intermediate to high silica rocks, such as those found in the SRB. Given the evolved nature of some of the samples, ratios and concentrations of trace elements and REEs are likely to reflect fractional crystallization and potentially crustal assimilation during magma ascent.

The concave-up, normalized REE diagrams for the andesitic and dacitic samples suggests pyroxene and amphibole fractionation (Fig. 7). The fractional crystallization of apatite is evident in both the older and younger SRB samples from the negative P anomalies seen in primitive mantle normalized spider diagrams. SRB volcanic rocks do not show a significant Eu negative anomaly; the lack of

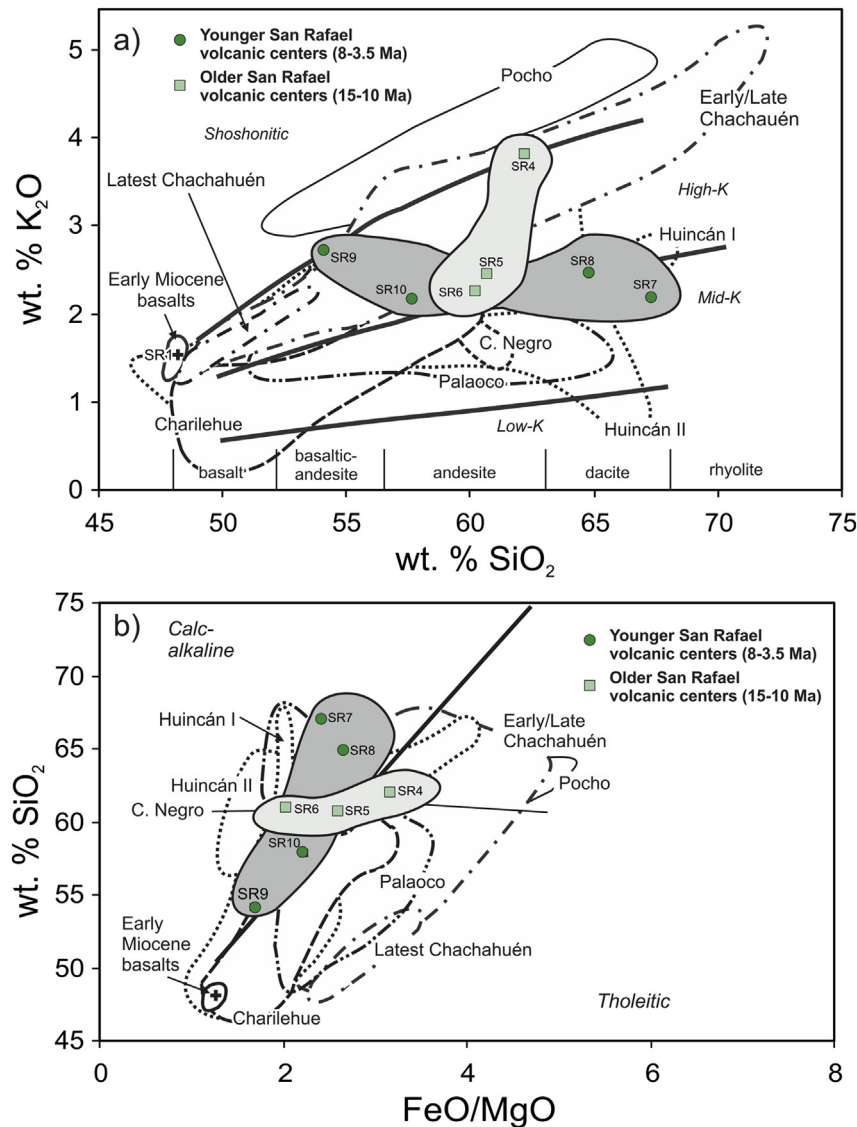


Fig. 6. Major element plots for the mesosilicic sequences of the San Rafael Block. a) K₂O vs. SiO₂. Note that most of the samples plot in the high-K field; b) SiO₂ vs. FeO/MgO. Note the calc-alkaline trend for the entire intermediate sequences in the San Rafael block. Other magmatic suites in the region are included for comparison (Kay and Gordillo, 1994; Kay et al., 2006a,b; Nullo et al., 2002; Spagnuolo et al., 2012; Dyhr et al., 2013a).

negative Eu-anomalies justifies the use of ratios involving Ba for the evolved rocks as it indicates limited fractional crystallization of plagioclase.

Lower crustal contamination could also be an explanation for low REE, Cs, Rb, Th and U contents and high values of Sr and Ba, such as seen in the more silica-rich lavas (samples SR7 and SR8), which also show Mg# similar to the more mafic lavas (29 and 28 for 64.89 and 67.17 wt.% SiO₂, for SR7 and SR8 respectively).

The andesitic to dacitic volcanic rocks from the San Rafael Block correspond to a high-K, calc-alkaline sequence as shown by their SiO₂, K₂O and FeO/MgO contents (Fig. 6). The Ba/La (>16) and La/Ta ratios (>25), as well as the Ba/Ta ratios, which are greater than 450, indicate the influence of the subducting slab on the source of these arc magmas (e.g., Hickey et al., 1986) (Fig. 8a, Table 1). Evidence for the influence of the subducting slab on the magma source region is also provided in their trace element patterns (Fig. 7), which show depletions in HFSE (e.g., Nb, Ta, Zr) that are immobile in fluids, relative to LILE (e.g., Rb, Ba, Sr, Pb), which are partitioned into the hydrous fluids that enrich the melts in the asthenospheric mantle wedge.

An arc-like signature is also observed in the Th/Hf vs. Ta/Hf diagram (Fig. 9) as these ratios are good indicators for calc-alkaline arc sources and mantle enrichment sources, respectively (e.g. Kay et al., 2006b). Overall, none of the samples show contribution from an enriched mantle source, instead they all contain arc-related components (Fig. 8). In contrast, the composition of the early Miocene basalt (sample SR1) implies significantly enriched mantle contributions (Fig. 8). Trace element tectonic discrimination diagrams, such as Wood (1980), which consider Ta–Th–Hf contents, also show an arc affinity for the studied volcanic assemblage, whilst the early Miocene olivine basalts correspond to alkaline intraplate basalts.

7.2. Temporal relationship

Middle Miocene to early Pliocene mesosilicic volcanic sequences from the near back-arc and far back-arc are distributed all along and across the studied latitudes, between eastern Malargüe fold and thrust belt in the west, to the SRB in the east. The spatial distribution of ages (Fig. 2) shows a migration of arc-related volcanism to

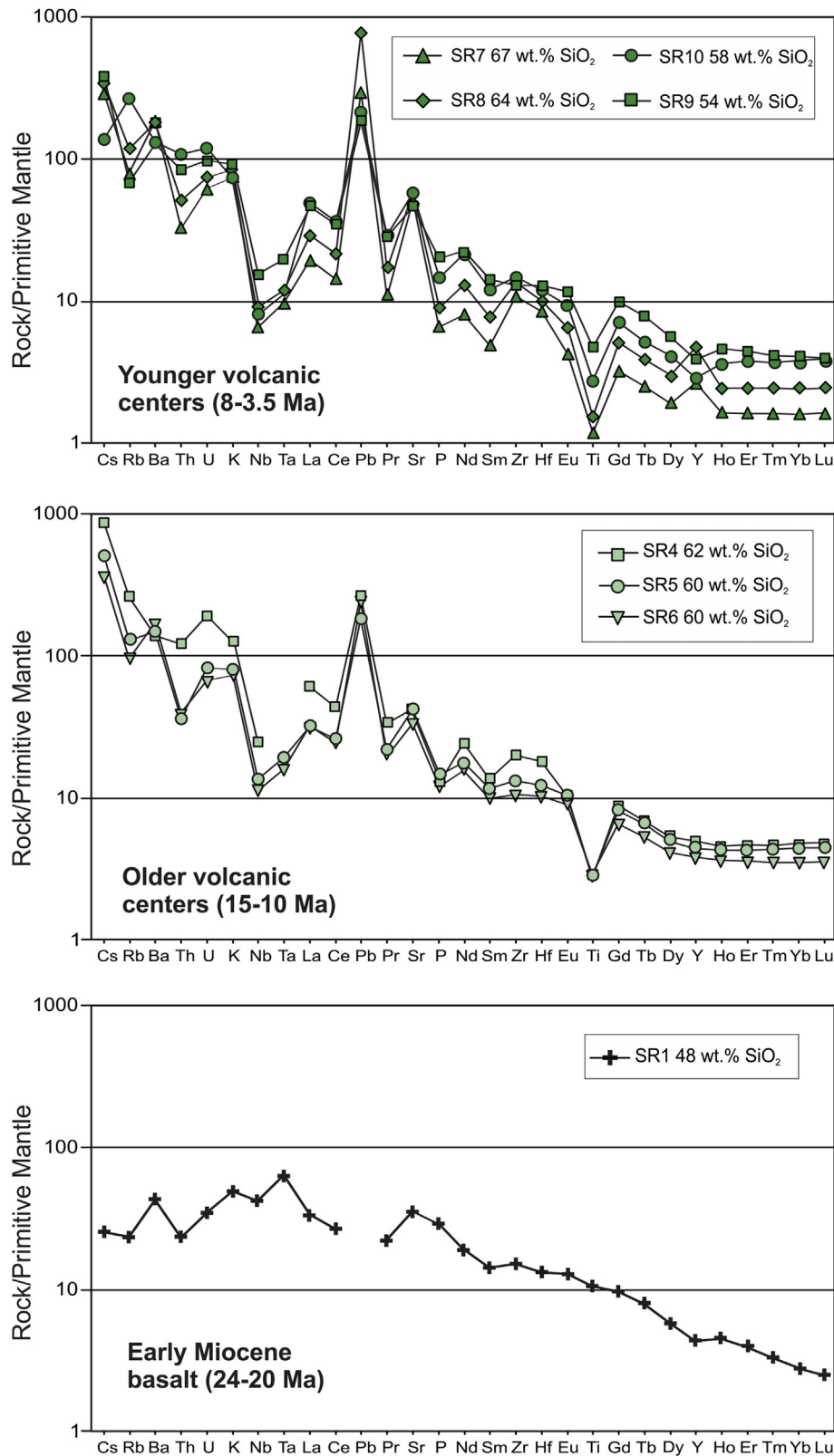
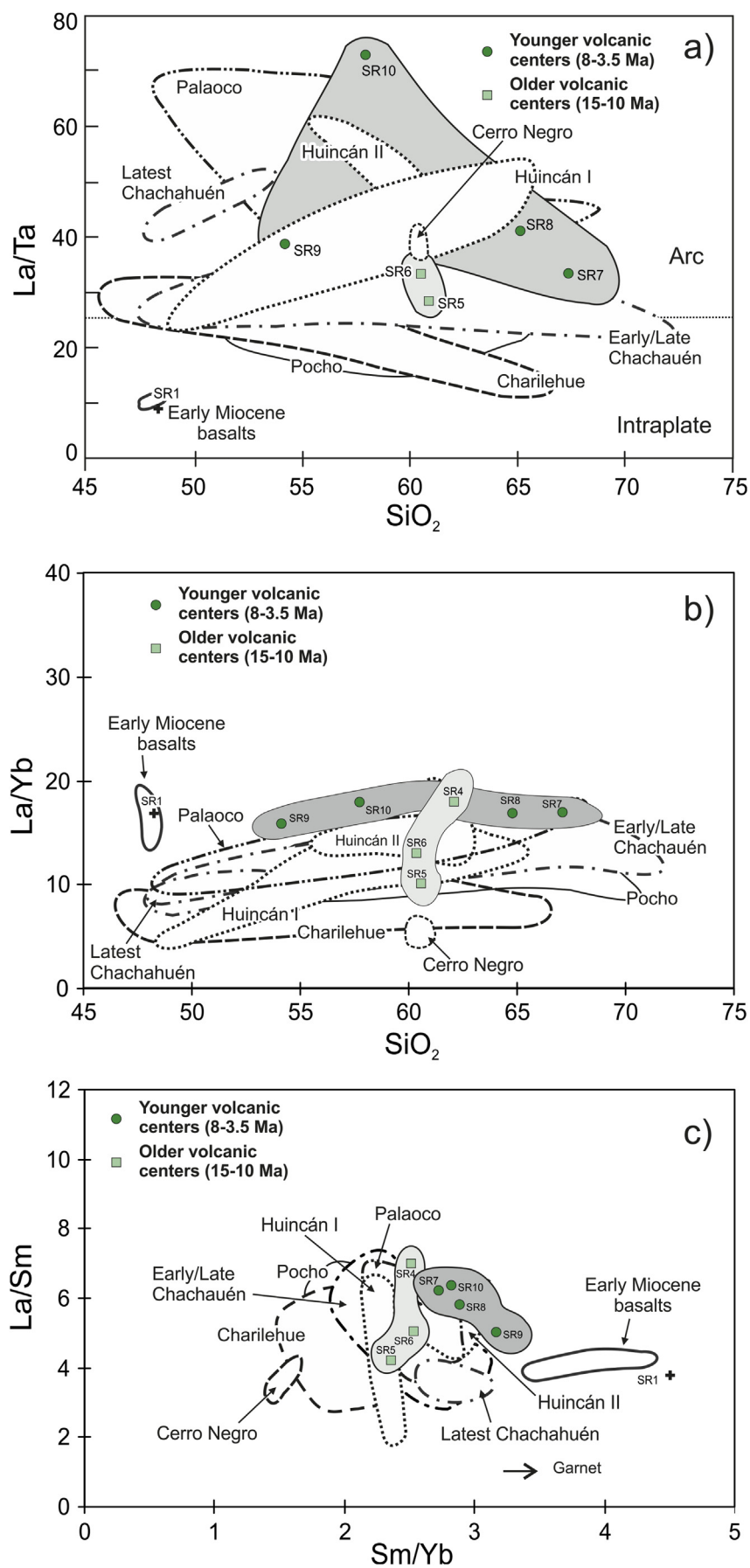


Fig. 7. Trace element spider diagrams for the late Miocene to early Pliocene intermediate sequences in the San Rafael Block, normalized to primitive mantle, (Sun and McDonough, 1989) show typical arc-related signatures. Samples correspond to the following volcanic centers: SR4-El Zaino, SR5-El Puntudo, SR6-El Chorroado, SR7 and SR8-Nevado-Plateado, SR9-Pelado, SR10-Los Cerritos.

the east from middle to late Miocene-early Pliocene (Nullo et al., 1993, 1999, 2002; Giambiagi et al., 2005, 2008; Kay et al., 2006a; Spagnuolo et al., 2012; Dyhr et al., 2013a,b; Ramos et al., 2014).

Volcanic sequences located in the near and far back-arc area can be included in two main volcanic stages, based on their age (Fig. 2): i) Middle to late Miocene, from 15 to 10 Ma, which includes



Huincán I and part of Huincán II andesites, Cerro Negro andesite, and Charilehue volcanic rocks (Nullo et al., 2002; Kay and Copeland, 2006; Kay et al., 2006a; Spagnuolo et al., 2012) and ii) latest Miocene to early Pliocene, from 8 to 3.5 Ma, which includes younger Huincán II andesites, Palaoco volcanism and Chachahuén Volcanic Complex (Nullo et al., 2002; Kay et al., 2006b; Dyhr et al., 2013a) (Figs. 2 and 3). Volcanism of SRB, located in the far back-arc, correlates with these stages: older San Rafael volcanic rocks overlap with the first 15 to 10 Ma period, while younger SRB rocks with the second phase, between 8 and 3.5 Ma; thus, they represent different stages of the evolution of the volcanism in the back-arc.

7.2.1. Middle to late Miocene volcanism

Middle to late Miocene magmas located in the back-arc show chemical signatures that are consistent with a source located in the mantle wedge above the slab and are therefore influenced by subducted components (Kay and Copeland, 2006; Kay et al., 2006b; Litvak et al., 2008, 2009). The 15–10 Ma stage of volcanism, represented by Huincán I and part of Huincán II lavas, Cerro Negro andesites and Charilehue volcanic rocks, has arc-like major and trace element compositions. However, geochemical differences between these units require variable arc settings. The Charilehue Formation, which corresponds to the oldest lavas in the 15–10 Ma stage, shows lower SiO_2 vs. FeO/MgO ratio when compared to the younger sequences within this stage (Fig. 6b). This indicates a more tholeiitic differentiation trend within the arc setting. Moreover, as reported by Spagnuolo et al. (2012), it has the lowest Ba/La and La/Ta ratios, while low La/Yb and Sm/Yb values are suggested to indicate a low pressure residual mineral assemblage in the source region. In comparison, Cerro Negro, and Huincán I and II lavas show more of an arc-related signature based on their Ba/La , La/Ta and Ta/Hf ratios than Charilehue Miocene lavas (Figs. 8 and 9) (Kay et al., 2006b; Dyhr et al., 2013a).

The geochemistry of the older San Rafael volcanic rocks (15–10 Ma) fits within this framework for middle to late Miocene magmatism in the Payenia back-arc. The calc-alkaline arc-like SRB rocks are distinctly different to the tholeiitic Charilehue Formation and early Miocene sequences (Fig. 6). Evidence of arc-related contributions is also seen in their Th/Hf vs. Ta/Hf diagram (Fig. 9) and particularly, by the low Ti contents and HFSE depletion in San Rafael volcanic rocks (Fig. 7). In agreement, Dyhr et al. (2013a) suggested that the late Miocene Palaoco volcanic sequences, exhibits a stronger arc-related geochemical signature when compared to the older volcanic events (e.g., Charilehue and Huincán), following the general trend towards an increase in slab-derived components present in back-arc magmas with time.

7.2.2. Latest Miocene to early Pliocene volcanism

The Chachahuén Volcanic Complex is located immediately south of the SRB (Fig. 2) volcanism and comprehends a magmatic activity which ranges from 7.3 to 4.9 Ma (Kay et al., 2006a). In order to evaluate the evolution of the latest Miocene volcanic rocks, it is useful to compare the geochemical characteristics of the younger SRB volcanism with the Chachahuén Volcanic Complex. Both volcanic sequences contain similar ages and petrographic features. According to Kay et al. (2006a) three main volcanic events can be identified within the Chachahuén Volcanic Complex. The first event, corresponding to the late Miocene Vizcachas Group, ranges

in age from 7.3 to 6.8 Ma and is composed of dacitic dikes along with andesitic to dacitic ignimbrites and lava flows that display intraplate chemical affinities. Even though this temporal volcanic stage is represented in the SRB study area, its composition does not indicate an intraplate affinity. The younger events described by Kay et al. (2006a) in the Chachahuén Volcanic Complex are the Early and Late Chachahuén groups. The Early Chachahuén Group has an age range of 6.8–6.4 Ma and includes an older sequence of intermediate composition (andesites to dacites) and a younger, more mafic sequence (basaltic to bas-andesitic dykes and lava flows). The Late Chachahuén Group is composed of an andesitic to dacitic pyroclastic unit overlain by basaltic to basandesitic lava flows, and hornblende-rich andesites; which range in age from 6.4 to 4.9 Ma (Kay et al., 2006a). The andesites and dacites of SRB volcanism share common petrographical characteristics with these two Chachahuén groups.

The chemical compositions of the Chachahuén volcanic groups are also, in general, similar to those of the SRB. Major element compositions of the SRB volcanic rocks plot within the Chachahuén fields; both series are high-K rocks (Fig. 6a) with calc-alkaline trends as shown by FeO/MgO ratios, although some of Chachahuén volcanics also plot in the tholeiitic field (Fig. 6b).

Arc-like affinities were also reported for the Chachahuén volcanic rocks (Kay et al., 2006a), for example as seen in their La/Ta ratios (Fig. 7a). A plot of Th/Hf vs. Ta/Hf (Fig. 9) also shows arc-derived contributions for both the Chachahuén and San Rafael volcanic sequences. Moreover, the Chachahuén volcanic rocks and the younger San Rafael rocks show the strongest arc-related signature when compared with earlier Miocene volcanism, based on their high Ba/Ta and La/Ta ratios (700–2000 and 27–50, respectively). The Chachahuén and SRB rocks also share a flattened overall REE pattern and similar La/Yb and Sm/Yb ratios. Although there is an overlap of both fields, as seen in Fig. 8, some of the Early/Late Chachahuén volcanic rocks have lower Sm/Yb ratios than the SRB rocks. The primary difference between the Chachahuén and SRB volcanic rocks is that the Chachahuén lavas display a small Eu anomaly (overall $\text{Eu}/\text{Eu}^* = 0.82\text{--}0.94$, Kay et al., 2006b) which is more pronounced in the silicic samples, while SRB rocks lack this feature (overall $\text{Eu}/\text{Eu}^* = 0.94\text{--}1.10$). The absence of an Eu anomaly in younger SRB rocks could reflect plagioclase accumulation in the SRB magmas. Alternatively, it could reflect more oxidizing conditions for SRB volcanism or plagioclase fractionation inhibited in magmas with high water content (Muntener et al., 2001).

7.3. The evolution and expansion of the Payenia shallow subduction zone

By constraining the spatial distribution, age and geochemical signatures of the volcanic units located in the near to far Payenia back-arc, an increased understanding can be gained into the influence of the subducting slab on the composition of arc magmas, the location and expansion of the arc over time, and the development of the Payenia shallow subduction zone. Charilehue volcanic rocks (15–14 Ma) record the earliest and westernmost position of slab influence on a near to middle back-arc position in the region, which can be correlated with Huincán I, part of Huincán II and the Cerro Negro Andesite, with a time range of 14–10 Ma (Figs. 2 and 10a). It is important to notice, however, that some slab-derived

Fig. 8. a) La/Ta ratio vs. SiO_2 diagram for volcanic rocks in the Payenia back-arc that shows La/Ta ratios indicative of arc settings for middle Miocene to early Pliocene sequences. b) La/Yb ratio vs. SiO_2 . Note that most of the intermediate sequences in the San Rafael Block have relatively high values compared to regionally and temporally related magmatism; c) Light rare earth elements (La/Sm) vs. heavy rare elements (Sm/Yb). Note that the younger, intermediate samples in the San Rafael Block have slightly higher Sm/Yb ratios than the Chachahuén volcanic rocks, which are located at the southernmost extent of the proposed shallow subduction zone. Data from Huincán I, II, Chachahuén, Charilehue, Cerro Negro and Palaoco are from Nullo et al. (2002), Kay et al. (2006a,b), Spagnuolo et al. (2012) and Dyhr et al., (2013a).

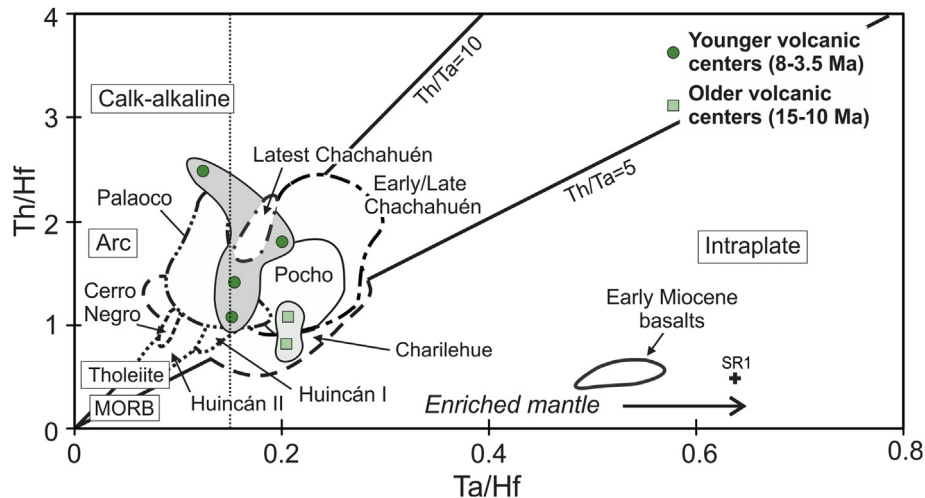


Fig. 9. Th/Hf vs. Ta/Hf ratios. Note that intermediate sequences of the San Rafael Block show Ta/Th ratios more related to arc values, such as the regionally related Miocene magmas (Nullo et al., 2002; Kay et al., 2006a,b; Spagnuolo et al., 2012; Dyhr et al., 2013a). Contrastingly, early Miocene basalts in the same region show intraplate-related values. Data for the Pocho volcanic field is from Kay and Gordillo (1994).

components were also identified in the Sierra de Huantraico lavas (e.g., Cerro Bayo volcano, 18–16 Ma) which are located slightly to the south and east of the SRB volcanic rocks (Fig. 2). These lavas represent the first evidence for the influence of the slab on a back-arc position in the Neuquén basin at around 20 Ma (Kay and Copeland, 2006; Dyhr et al., 2013b). Therefore, Kay et al. (2006b) had suggested the initial development of the shallow subduction zone in this area after 20 Ma, more clearly between 18 and 10 Ma, when the arc signature becomes stronger. This is based on the presence of andesitic eruptions in a back-arc position from 18 to 17 Ma, whose geochemical features are consistent with subducted components influencing a mantle wedge above a subducting slab

(Kay et al., 2006b). The older SRB volcanic rocks (15–10 Ma), whose distribution shows a marked inflection at 36°S towards the east, with respect to the zone of arc expansion, display chemical compositions characterized by an influence of slab derived fluids. Arc expansion continued between 10 and 6 Ma and is recorded by the younger San Rafael volcanic rocks (8–3.5 Ma). After ~4 Ma no volcanism with clear arc-related signatures was developed in the back-arc at these latitudes (Figs. 2 and 10b).

Based on the distribution, ages and geochemical features of arc-related products emplaced in the back-arc position in southern Mendoza (Fig. 2), the youngest lavas of the Chachahuén Volcanic Complex (4.9 Ma) had previously been considered to represent the

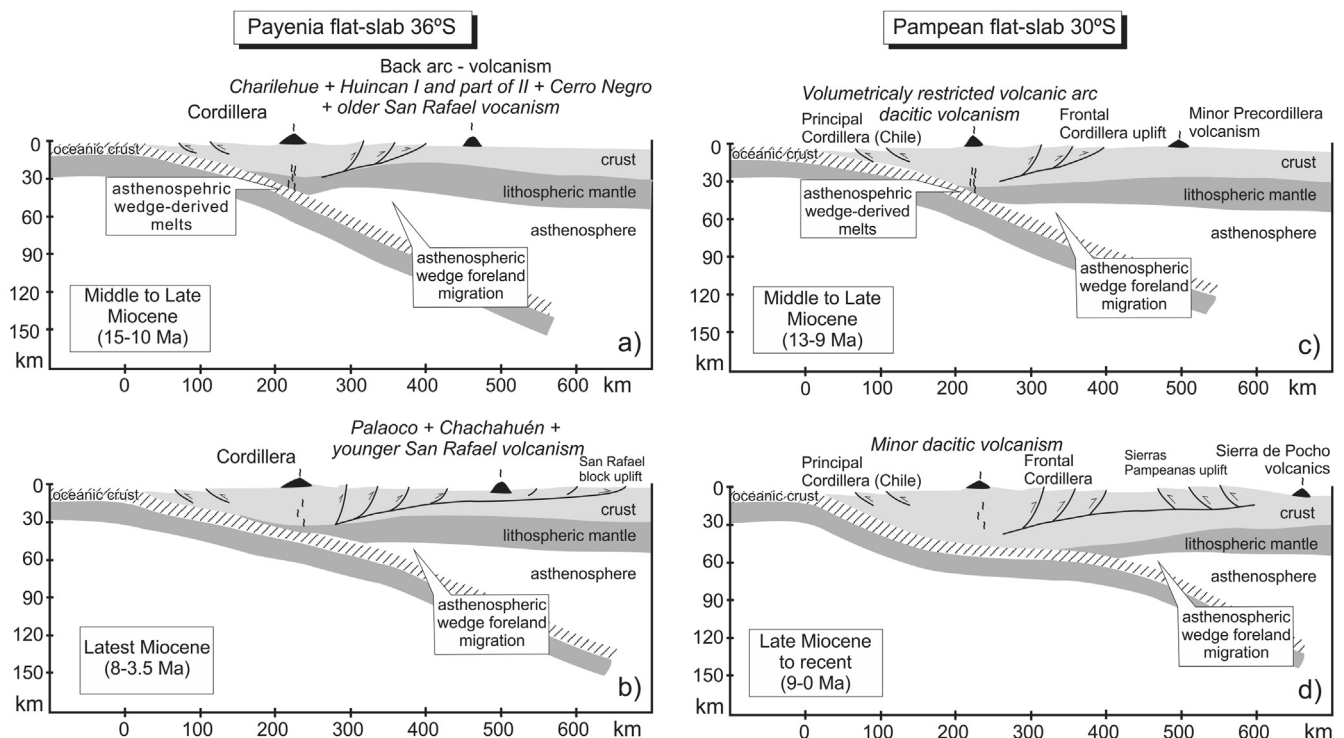


Fig. 10. Cross sections showing the main magmatic events during the Miocene, for the Payenia shallow subduction zone at 36°S (a and b), compared to cross sections at 30°S for the Pampean flat-slab segment (c and d) (modified from Litvak et al., 2007). Note that no active volcanism is present over the modern Pampean flat-slab segment.

easternmost extent of the shallow subduction regime (Kay et al., 2006a). Even though the San Rafael volcanic rocks analyzed in this work encompass the entire lifespan of the Chachahuén Volcanic Complex (Kay et al., 2006a,b), SRB volcanism has older components. The initial period of slab influence between 15 and 10 Ma represented by the older San Rafael volcanic rocks precedes the long-lived Chachahuén stratovolcano and indicates an older permanence of the arc magmatism in the back-arc zone. Additionally, the distribution of the younger San Rafael volcanism (8–3.5 Ma) suggests that the shallowly subducting slab had a greater eastern extent and extended to lower latitudes (i.e., further north) than previously observed.

Lateral expansion of the Payenia shallow subduction zone on the SRB shows a more eastward development than previously thought. However, location of younger volcanic centers, such as Pliocene Cerro Nevado-Plateado (located ~80 km east of Chachahuén) are actually located at a similar distance to the Chilean trench as the Chachahuén center (Figs. 1 and 10). This is explained by the inflexion of the geometry of the trench at these latitudes.

Finally, the evolution of the Payenia shallow subduction segment can be compared with the Pampean flat-slab segment located immediately to the north (33°30'–27°S) (Fig. 1) (Kay et al., 1991; Kay and Abruzy, 1996).

Kay et al. (2006a,b) discussed the geometry of the slab and the development of shallow subduction during the late Miocene in both shallow subduction segments. They consider shallow subduction to be less pronounced for the Payenia shallow subduction zone segment, as the Chachahuén Complex is located only 500 km away from the trench, while the Pocho volcanic field, whose magmatism show arc-related signatures in the Pampean flat-slab retroarc (Kay and Gordillo, 1994), is ~700 km away. The data we present here for volcanic rocks from the SRB indicates that slab-influenced magmatism developed 480–500 km away from the Chile trench, at ~36°S (Fig. 10), but earlier than previously thought (~15 Ma).

A further difference between the Payenia shallow subduction zone and the Pampean flat-slab segment relates to the potential increase in crustal thickness that could have occurred in both settings, and which should be reflected in the observed geochemical features. Kay et al. (2006a,b) suggest that the Early/Late Chachahuén magmas show similarities with the late Miocene Pocho volcanic field. They share the same high-K field in the K₂O vs. SiO₂ diagram, REE patterns with overlapping La/Yb, La/Sm and Sm/Yb ratios and ratios of La/Ta, Ba/La and Ta/Hf typical for arc-derived lavas. SRB volcanism share similar geochemical compositions, with slightly higher La/Yb and Sm/Yb ratios and less enrichment in K₂O (Figs. 6 and 8).

Kay et al. (2006b) pointed out that the crustal thickness, based on geophysical criteria, in the Main Cordillera above the Pampean flat-slab segment (~30°S), is in the order of 60–70 km while it is close to 40–45 km at 36°S. Crustal thicknesses in the Main Cordillera over the Pampean flat-slab segment explains the high Sm/Yb values (>4) of the Late Miocene volcanic rocks present in the region (e.g., Kay et al., 1991, 1999; Litvak et al., 2007), which would suggest that magmas were equilibrated with garnet as a residual mineral phase. The presence of garnet as a residual phase is indicative of high melting pressure, which can be attributed to an increase in lithospheric thickness due to crustal shortening in a compressional setting. In comparison, neither Chachahuén lavas nor SRB volcanic rocks in the Payenia region show Sm/Yb that could reflect garnet as a residual mineral phase (Fig. 8b), which implies a lithosphere of normal thickness (40–45 km) was present in the foreland region during the middle Miocene to early Pliocene (Fig. 10).

8. Concluding remarks

Miocene to Pliocene magmatism located in the back-arc in the Payenia region within the SRB comprises andesitic to dacitic volcanic centers whose products show typical high-K, calc-alkaline compositions and trace elements patterns that display arc-like signatures. Two stages of arc-related volcanism can be recognized: a first stage that corresponds to the oldest volcanic centers (15–10 Ma) and a second one, which consists of the younger volcanic centers (8–3.5 Ma). The spatio-temporal relationship between volcanic centers and their geochemistry appears to document the shallowing of the subducting slab and the formation of the Payenia shallow subduction segment at these latitudes. Regionally, SRB volcanism can be related to the middle Miocene to early Pliocene arc expansion from the near back-arc to the far back-arc whose volcanism show an increase of typical arc-related chemical signature components.

San Rafael magmatism reflects the maximum development of the Payenia shallow-angle subduction zone between 15 and 4 Ma. The shallower-slab had started to develop by 18 Ma to the south of the SRB area, and then expanded to the north as the arc activity reached the SRB between 15 and 10 Ma, then expanding even further to the north and south. Finally, the volcanic activity remained in this foreland area, until 4 Ma, whose magmas represent the easternmost influence of the Payenia shallow subduction zone in the area.

Acknowledgments

The authors acknowledge the financial support from CONICET (grant 11420110100) and University of Buenos Aires (grant UBACYT 20020120200090BA). The authors thanks Drs. S. Kay and P. Leal for fruitful discussion on the subject. We also thank three anonymous reviewers for their constructive comments. This is paper number 168 of the Instituto de Estudios Andinos Don Pablo Groeber.

Appendix A. Supplementary data

Supplementary data related to this article can be found at <http://dx.doi.org/10.1016/j.jsames.2015.09.010>.

References

- Baldauf, P., 1997. Timing of the Uplift of the Cordillera Principal, Mendoza Province, Argentina. George Washington University, p. 356 (M.S. thesis).
- Bermúdez, A., 1991. Sierra del Nevado. El límite oriental del arco volcánico del Neógeno entre los 35°30' y 36° L.S. Argentina. In: VI° Congreso Geológico Chileno (Santiago de Chile), Actas, vol. 1, pp. 318–322.
- Bermúdez, A., Delpino, D., 1989. La Provincia Basáltica Andino Cuyana (35–37°L.S.). Rev. Asoc. Geol. Argent. 44 (1–4), 35–55.
- Bermúdez, A., Delpino, D., Frey, F., Saal, A., 1993. Los basaltos de retroarco extra-andinos. In: Ramos, V.A. (Ed.), Geología y Recursos Naturales de Mendoza. XII° Congreso Geológico Argentino y II° Congreso de Exploración de Hidrocarburos (Buenos Aires), Relatorio I-13, pp. 161–172.
- Bertotto, G.W., Cingolani, C.A., y Bjerg, E.A., 2009. Geochemical variations in Cenozoic back-arc basalts at the border of La Pampa and Mendoza provinces, Argentina. J. S. Am. Earth Sci. 28, 360–373.
- Burns, W.M., Jordan, T., Copeland, P., Kelley, S., 2006. Extensional tectonics in the Oligo-Miocene Southern Andes as recorded in the Cura-Mallín basin. In: Kay, S.M., Ramos, V.A. (Eds.), Evolution of an Andean Margin: a Tectonic and Magmatic View From the Andes to the Neuquén Basin (35–39°S). Geological Society of America, pp. 163–184 (Special Paper 407).
- Charrier, R., Baeza, O., Elgueta, S., Flynn, J., Gans, P., Kay, S., Muñoz, N., Wyss, A., Zurita, E., 2002. Evidence for Cenozoic extensional basin development and tectonic inversión south of the flat-slab segment, southern Central Andes, Chile (33°–36°S). J. S. Am. Earth Sci. 15, 117–139.
- Cobbold, P.R., Rosello, E.A., 2003. Aptian to recent compressional deformation, foothills of the Neuquén Basin Argentina. Mar. Pet. Geol. 20, 429–443.
- Croft, D., Radic, J., Zurita, E., Charrier, R., Flynn, J., Wyss, A., 2003. A Miocene toxodontid (Mammalia: Notoungulata) from the sedimentary series of the Cura-Mallín Formation, Lonquimay Chile. Rev. Geol. Chile 30, 285–298.

- Delpino, D.H., Bermúdez, A., 1985. Volcán Plateado. Vulcanismo andesítico de retroarco en el sector extraandino de la Provincia de Mendoza, 35°42' Lat. Sur. Argentina. In: IV° Congreso Geológico Chileno (Antofagasta), Actas, vol. 3, pp. 108–119.
- Desanti, R., 1956. Hoja Cerro Diamante. 1 sheet 1: 200,000. Provincia de Mendoza. Servicio Nacional Minero Geológico, Boletín, Buenos Aires.
- Dyhr, C.T., Holm, P.M., Llambías, E.J., 2013a. Geochemical constraints on the relationship between the Miocene–Pliocene volcanism and tectonics in the Palao and Fortunoso volcanic fields, Mendoza Region, Argentina: new insights from $^{40}\text{Ar}/^{39}\text{Ar}$ dating, Sr–Nd–Pb isotopes and trace elements. *J. Volcanol. Geotherm. Res.* 266, 50–68.
- Dyhr, C.T., Holm, P.M., Llambías, E.J., Scherstén, A., 2013b. Subduction controls on Miocene back-arc lavas from Sierra de Huantraico and La Matancilla and new $^{40}\text{Ar}/^{39}\text{Ar}$ dating from the Mendoza Region, Argentina. *Lithos* 179, 67–83.
- Fidalgo, F., 1973. Hoja Llancanelo, 1 sheet 1: 250,000. Provincia de Mendoza. Servicio Nacional Minero Geológico, Boletín, Buenos Aires.
- Flynn, J., Charrier, R., Croft, D., Gans, P., Herriott, T., Wertheim, J., Wyss, A., 2008. Chronologic implications of new Miocene mammals from the Cura Mallín and Trapa Formations, Laguna del Laja area, south Central Chile. *J. S. Am. Earth Sci.* 26 (4), 412–423.
- Fock, A., 2005. Cronología y tectónica de la exhumación en el Neógeno de los Andes de Chile Central entre los 33° y los 34°S (M.S. thesis). Universidad de Chile, Santiago Chile, p. 235.
- Fock, A., Charrier, R., Maksae, V., Farías, M., Alvarez, P., 2006. Evolución cenozoica de los Andes de Chile Central. In: XI° Congreso Geológico Chileno (Antofagasta), Abstracts, vol. 2, pp. 205–208.
- Folguera, A., Naranjo, J.A., Orihashi, Y., Sumino, H., Nagao, K., Polanco, E., Ramos, V.A., 2009. Retroarc volcanism in the northern San Rafael Block (34°–35°30'S), southern Central Andes: occurrence, age, and tectonic setting. *J. Volcanol. Geotherm. Res.* 186, 169–185.
- Galland, O., Hallot, E., Cobbold, R., Ruffet, G., Brémond d'Ar, J., 2005. Coeval volcanic activity and tectonic shortening, Tromen volcano, Neuquén province, Argentina. In: VI° International Symposium on Andean Geodynamics, Extended Abstracts, pp. 293–296.
- Giambiagi, L.B., Bechis, F., García, V., Clark, A., 2005. Temporal and spatial relationship between thick- and thin-skinned deformation in the thrust front of the Malargüe fold and thrust belt, Southern Central Andes. In: VI° International Symposium on Andean Geodynamics, Extended Abstracts, pp. 315–318.
- Giambiagi, L., Bechis, F., García, V., Clark, A., 2008. Temporal and spatial relationship between thick- and thin-skinned deformation in the Malargüe fold and thrust belt, Southern Central Andes. *Tectonophysics* 459, 123–139.
- Godoy, E., Yañez, G., Vera, E., 1999. Inversion of an Oligocene volcano tectonic basin and uplifting of its superimposed Miocene magmatic arc in the Chilean Central Andes: first seismic and gravity evidences. *Tectonophysics* 306, 217–236.
- González Díaz, E.F., 1964. Rasgos geológicos y evolución geomorfológica de la Hoja 27 d (San Rafael) y zona occidental vecina (Provincia de Mendoza). *Rev. Asoc. Geol. Argent.* 19, 151–188.
- González Díaz, E.F., 1972a. Descripción geológica de la Hoja 27d San Rafael, Provincia de Mendoza. *Serv. Nac. Min. Geol. Bol.* 132, 1–127.
- González Díaz, E.F., 1972b. Descripción geológica de la Hoja 30d Payún-Matrú, Provincia de Mendoza. *Dir. Nac. Geol. Min. Bol.* 130, 1–88.
- González Díaz, E.F., 1972c. Descripción geológica de la Hoja 30e Agua Escondida, Provincia de Mendoza. *Dir. Nac. Geol. Min. Bol.* 135, 1–79.
- González Díaz, E.F., 1979. Descripción geológica de la Hoja 31d La Matancilla, Provincia de Mendoza. *Dir. Nac. Geol. Min. Bol.* 173, 1–93.
- Groeber, P., 1946. Observaciones geológicas a lo largo del meridiano 70, I. Hoja Chos Malal. *Rev. Soc. Geol. Argent.* 1, 177–208.
- Gudnason, J., Holm, P.M., Seager, N., Llambías, E.J., 2012. Geochronology of the late Pliocene to recent volcanic activity in the Payenia back-arc volcanic province, Mendoza Argentina. *J. S. Am. Earth Sci.* 37, 191–201.
- Hernando, I.R., Llambías, E.J., González, P.D., Sato, K., 2002. Volcanic stratigraphy and evidence of magma mixing in the Quaternary Payún Matrú volcano, Andean backarc in western Argentina. *Andean Geol.* 39 (1), 158–179.
- Hernando, I.R., Aragón, E., Frei, R., González, P.D., Spakman, W., 2014. Constraints on the origin and evolution of the magmas in the Payún Matrú Volcanic Field, Quaternary Andean Back-arc of Western Argentina. *J. Pet.* 55 (1), 209–239.
- Hickey, R.L., Frey, F.A., Gerlach, D.C., López Escobar, L., 1986. Multiple sources for basaltic arc rocks from the Southern Volcanic Zone of the Andes (34°–41°S): trace elements and isotopic evidence for contributions from subducted oceanic crust, mantle and continental crust. *J. Geophys. Res.* 91, 5963–5983.
- Holmberg, E., 1962. Descripción geológica de la Hoja 32d, Chachahuén, Prov. de Neuquén y Mendoza. *Dir. Nac. Geol. Min. Bol.* 91, 1–72.
- Holmberg, E., 1964. Descripción geológica de la Hoja 33d, Auca Mahuida, Provincia del Neuquén. *Dir. Nac. Geol. Min. Bol.* 94, 1–88.
- Holmberg, E., 1973. Descripción geológica de la Hoja 29d, Cerro Nevado, Provincia de Mendoza. *Dir. Nac. Geol. Min. Bol.* 144, 1–71.
- Jordan, T.E., Isacks, B., Ramos, V.A., Allmendinger, R.W., 1983. Mountain building in the Central Andes. *Episodes* 3, 20–26.
- Kay, S.M., Abruzzi, J.M., 1996. Magmatic evidence for Neogene lithospheric evolution of the central Andean flat-slab between 30°S and 32°S. *Tectonophysics* 259, 15–29.
- Kay, S.M., Copeland, P., 2006. Early to middle Miocene backarc magmas of the Neuquén Basin: geochemical consequences of slab shallowing and the westward drift of South America. In: Kay, S.M., Ramos, V.A. (Eds.), *Late Cretaceous to Recent Magmatism and Tectonism of the Southern Andean Margin at the Latitude of the Neuquén Basin* (36°–39°S). Geological Society of America, pp. 185–214 (Special Paper 407).
- Kay, S.M., Gordillo, C.E., 1994. Pocho volcanic rocks and the melting of depleted continental lithosphere above a shallowly dipping subduction zone in the central Andes. *Contrib. Mineral. Pet.* 117, 25–44.
- Kay, S.M., Mpodozis, C., Ramos, V.A., Munizaga, F., 1991. Magma source variations from mid to late Tertiary volcanic rocks erupted over a shallowing subduction zone and through a thickening crust in the Main Andean Cordillera (28°–33°S). In: Harmin, R.S., Rapela, C. (Eds.), *Andean Magmatism and its Tectonic Setting*. Geological Society of America, pp. 113–137 (Special Paper 265).
- Kay, S.M., Mpodozis, C., Coira, B., 1999. Neogene magmatism, tectonism and mineral deposits of the Central Andes (22°–23°S Latitude). In: Skinner, B.J. (Ed.), *Geology and Ore Deposits of the Central Andes*. Society of Economic Geologists, pp. 27–59 (Special Publication 7).
- Kay, S.M., Mancilla, O., Copeland, P., 2006a. Evolution of the Backarc Chachahuén volcanic complex at 37°S latitude over a transient Miocene shallow subduction zone under the Neuquén Basin. In: Kay, S.M., Ramos, V.A. (Eds.), *Late Cretaceous to Recent Magmatism and Tectonism of the Southern Andean Margin at the Latitude of the Neuquén Basin* (36°–39°S). Geological Society of America, pp. 215–246 (Special Paper 407).
- Kay, S.M., Burns, W.M., Copeland, P., Mancilla, O., 2006b. Upper Cretaceous to Holocene magmatism and evidence for transient Miocene shallowing of the Andean subduction zone under the northern Neuquén Basin. In: Kay, S.M., Ramos, V.A. (Eds.), *Late Cretaceous to Recent Magmatism and Tectonism of the Southern Andean Margin at the Latitude of the Neuquén Basin* (36°–39°S). Geological Society of America, pp. 19–60 (Special Paper 407).
- Le Maitre, R.W., Bateman, P., Dudek, A., Keller, J., Lameyre, M.J., Le Bas, P.A., Sabine, R., Schmid, H., Sorensen, A., Streckeisen, A.R., Wooley Zanettin, B., 1989. *A Classification of Igneous Rocks and Glossary of Terms*. Blackwell, Oxford, p. 193.
- Litvak, V.D., Poma, S., Kay, S.M., 2007. Paleogene and Neogene magmatism in the Valle del Cura region: a new perspective on the evolution of the Pampean flat slab, San Juan province, Argentina. *J. S. Am. Earth Sci.* 24, 117–137.
- Litvak, V., Folguera, A., Ramos, V., 2008. Determination of an arc-related signature in Late Miocene volcanism over the San Rafael Block, Southern Central Andes (34°30'–37°) Argentina: the Payenia shallow subduction zone. In: VII° International Symposium on Andean Geodynamics, Extended Abstracts, pp. 289–291.
- Litvak, V., Folguera, A., Ramos, V., 2009. La expansión hacia el antepaís del arco volcánico mioceno al sur de la provincia de Mendoza, Andes Centrales del Sur. In: XII° Congreso Geológico Chileno (Santiago de Chile), p. S9:041.
- Llambías, E.J., Bertotto, G.W., Risso, C., Hernando, I., 2010. El volcanismo cuaternario en el retroarco de Payenia: una revisión. *Rev. Asoc. Geol. Argent.* 67 (2), 278–300.
- Marshall, L., Drake, R., Curtiss, G., 1986. 40K–40Ar calibration of late Miocene–Pliocene Mammal-bearing Hayuerías and Tunuyán Formations, Mendoza Province, Argentina. *J. Paleontol.* 60, 448–457.
- Muñoz Bravo, J., Stern, C., Bermúdez, A., Delpino, D., Dobbs, M.F., Frey, F.A., 1989. El volcanismo plio-cuaternario a través de los 38° y 39°S de los Andes. *Rev. Asoc. Geol. Argent.* 44, 270–286.
- Muntener, O., Kelemen, P., Grove, T., 2001. The role of H₂O during crystallization of primitive arc magmas under uppermost mantle conditions and genesis of igneous pyroxenites: an experimental study. *Contrib. Mineral. Pet.* 141, 643–658.
- Nulló, F.E., Franchi, M., González, P., Herrero, J.C., Reinoso, M.S., 1993. Mapa Geológico de la Provincia de Río Negro. Dirección Nacional del Servicio Geológico, Buenos Aires.
- Nulló, F.E., Panza, J.L., Blasco, G., 1999. El Jurásico y Cretácico de la Cuenca Austral. In: Caminos, R. (Ed.), *Geología Argentina*. Servicio Geológico Minero Argentino, pp. 528–535.
- Nulló, F.E., Stephens, G., Otamendi, J., Baldauf, P., 2002. El volcanismo del Terciario superior del sur de Mendoza. *Rev. Asoc. Geol. Argent.* 57 (2), 119–132.
- Núñez, E., 1976a. Descripción geológica de la Hoja 31e Chical-Co, Provincia de Mendoza. *Dir. Nac. Geol. Min. Bol.* 1–92.
- Núñez, E., 1976b. Descripción geológica de la Hoja 28c El Nihuil, Provincia de Mendoza. *Dir. Nac. Geol. Min. Bol.* 1–100.
- Núñez, E., 1979. Descripción geológica de la Hoja 28d Estación Soitú, Provincia de Mendoza. *Dir. Nac. Geol. Min. Bol.* 166, 1–67.
- Ostera, H., Linares, E., Haller, M., 1999. Paramillos Altos intrusive belt, southern Mendoza, Argentina. Ages, chemical and isotopic constraints. In: II° South American Symposium on Isotope Geology, Actas, pp. 256–260.
- Polanski, J., 1963. Estratigrafía, neotectónica y geomorfología del Pleistoceno pedemontano, entre los ríos Diamante y Mendoza. *Rev. Asoc. Geol. Argent.* 17, 127–349.
- Polanski, J., 1964. Descripción geológica de la Hoja 26c, La Tosca (Prov. de Mendoza). *Dir. Nac. Geol. Min. Bol.* 101, 1–86.
- Quidelleur, X., Carlut, J., Tchilinguirian, P., Germa, A., Gillot, P.-Y., 2009. Paleomagnetic directions from mid-latitude sites in the southern hemisphere (Argentina): contribution to time averaged field models. *Phys. Earth Planet. Inter.* 172, 199–209.
- Radici, J.P., Rojas, L., Carpinelli, A., Zurita, E., 2002. Evolución Tectónica de la cuenca Terciaria de Cura-Mallín Región Cordillerana Chileno Argentina (36°30'–39°00'S). In: XIV° Congreso Geológico Argentino (Calafate), Actas, vol. 3, pp. 233–237.
- Ramos, V.A., Barbieri, M., 1989. El volcanismo cenozoico de Huantraico: edad y

- relaciones isotópicas iniciales, provincia del Neuquén. *Rev. Asoc. Geol. Argent.* 43, 210–223.
- Ramos, V.A., Folguera, A., 2005a. Tectonic evolution of the Andes of Neuquén: constraints derived from the magmatic arc and foreland deformation. In: Veiga, G., Spalletti, L., Howell, J., Schwarz, E. (Eds.), *The Neuquén Basin: a Case Study in Sequence Stratigraphy and Basin Dynamics*. Geological Society of London, pp. 15–35 (Special Publication 252).
- Ramos, V.A., Folguera, A., 2005b. Structural and magmatic responses to steepening of a flat subduction: southern Mendoza, Argentina. In: VI^o International Symposium of Andean Geodynamics, Extended Abstracts, pp. 592–595.
- Ramos, V.A., Folguera, A., 2011. Payenia volcanic province in the Southern Andes: an appraisal of an exceptional Quaternary tectonic setting. *J. Volcanol. Geotherm. Res.* 201, 53–64.
- Ramos, V.A., Cristallini, E., Pérez, D.J., 2002. The Pampean flat-slab of the Central Andes. *J. S. Am. Earth Sci.* 15, 59–78.
- Ramos, V.A., Folguera, A., Litvak, V.D., Spagnuolo, M., 2014. Andean tectonic cycle: from crustal thickening to extension in a thin crust (34°–37°S). *Geosci. Front.* 5, 351–367.
- Rapela, C.W., Pankhurst, R.J., Casquet, C., Fanning, C.M., Baldo, E.-G., González-Casado, J.M., Galindo, C., Dahlquist, J., 2007. The Río de la Plata craton and the assembly of SW Gondwana. *Earth Sci. Rev.* 83 (1–2), 49–82.
- Rojas Vera, E.A., Selles, D., Folguera, A., Gimenez, M., Ruiz, F., Orts, D., Zamora Valcarce, G., Martínez, P., Bechis, F., Ramos, V.A., 2014. The origin of the Loncopué Trough in the retroarc of the Southern Central Andes from field, geophysical and geochemical data. *Tectonophysics* 637, 1–19.
- Rossello, E., Cobbold, P., Diraion, M., Arnaud, N., 2002. Auca Mahuida (Neuquén Basin, Argentina): a Quaternary shield volcano on a hydrocarbon-producing substrate. In: V^o International Symposium on Andean Geodynamics, Extended Abstracts, pp. 549–552.
- Søager, N., Holm, P.M., Llambías, E.J., 2013. Payenia volcanic province, southern Mendoza, Argentina: OIB mantle upwelling in a backarc environment. *Chem. Geol.* 349–350, 36–53.
- Soria, M.F., 1983. Vertebrados fósiles y edad de la Formación Aisol, provincia de Mendoza. *Rev. Asoc. Geol. Argent.* 38, 299–306.
- Spagnuolo, M., Litvak, V.D., Folguera, A., Ramos, V.A., 2012. Miocene magmatic expansion and mountain building at the southern Central Andes, 36°–37°S, Argentina. *J. Geodyn.* 53, 81–94.
- Suárez, M., Emparán, C., 1995. The stratigraphy, geochronology and paleogeography of a Miocene fresh-water interarc basin, southern Chile. *J. S. Am. Earth Sci.* 8, 17–31.
- Sun, S., McDonough, W.F., 1989. Chemical and isotopic systematics of oceanic basalts: implications for mantle composition and processes. In: Saunders, A.D., Norry, M.J. (Eds.), *Magmatism in the Ocean Basins*. Geological Society, pp. 313–345 (Special Publication 42).
- Wood, D.A., 1980. The application of Th-Hf-Ta diagram to problems of tectonomagmatic classification and to establishing the nature of crustal contamination of basaltic lavas of the British Tertiary volcanic province. *Earth Planet. Sci. Lett.* 50, 11–30.
- Yrigoyen, M.R., 1993. Los depósitos sinorogénicos terciarios. In: Ramos, V.A. (Ed.), *Geología y Recursos minerales de Mendoza*, Relatorio, vol. I(11), pp. 123–148.
- Yrigoyen, M.R., 1994. Revisión estratigráfica del Neógeno de las Huayquerías de Mendoza septentrional, Argentina. *Ameghiniana* 31, 125–138.